Macromolecules
ARTICLE

Macromolecules **2010**, *43*, 5149–5157 **5149**
DOI: 10.1021/ma100460y

Protein-Like Copolymers (PLCs) as Compatibilizers for Homopolymer Blends

Ravish Malik, Carol K. Hall, and Jan Genzer*

Department of Chemical & Biomolecular Engineering North Carolina State University Raleigh, North Carolina 27695-7905

Received February 26, 2010; Revised Manuscript Received April 23, 2010

ABSTRACT: We present the results of discontinuous molecular dynamics (DMD) computer simulations aimed at understanding the role of protein-like copolymers (PLCs) as compatibilizing agents for a polymer blend containing two incompatible homopolymers. The effectiveness of PLCs to act as compatibilizers is compared with that of block, alternating, and random copolymers at low copolymer concentration (~0.66%). PLCs localize at the interface and are preferentially oriented parallel to it, judged by comparing the parallel and perpendicular components of the radius of gyration ($\langle R_g^2\rangle_\parallel > \langle R_g^2\rangle_\perp$). At lower temperatures, PLCs possess higher interfacial width as they penetrate the interface more than random and alternating copolymers; the PLCs are very efficient at making multiple connection points across the interface. The average fraction of crossings for PLCs is as high as 80% of the number of junction points, that is, the number of bonds between A and B monomers in the AB copolymer. High-molecular-weight PLCs are likely to outperform random and alternating copolymers as efficient interfacial stabilizers.

Introduction

Polymer blending represents a cost-effective method for formulating new soft materials. The properties of polymer blends can be fine-tuned by varying the composition and the types of polymers that are mixed. However, polymer blending is challenging because polymers are usually chemically incompatible. Because the low entropic gain upon mixing cannot compensate the enthalpic losses due to unfavorable interactions, most polymer blends tend to macrophase separate, thereby limiting their potential applications. Macromolecular compatibilizers are typically added to overcome these difficulties. They segregate preferentially at the interface between the two immiscible homopolymers, thereby reducing interfacial tension and increasing structural integrity and homogeneity, leading to improved stability and mechanical strength of the interface. Whereas block copolymers have been used readily to improve the properties of immiscible polymer interfaces, a few studies suggested that random copolymer may, under certain circumstances, act as effective compatibilizing agents as well. In this article, we discuss how the compatibilization efficacy of random copolymers can be tuned by adjusting the comonomer sequences.

Protein-like copolymers (PLCs) represent a new class of functional copolymer that exhibits large-scale compositional heterogeneities and long-range correlations along the comonomer sequence.[1−3] The concept of PLCs was first introduced by Khokhlov and coworkers,[2,3] who used computer simulations to demonstrate that random copolymers with tunable monomer sequences could be generated by adjusting the compactness of a parent homopolymer composed of component A and then converting exposed segments on the polymer surface into B segments by reacting them with other species in the surrounding solution. In a series of papers, Khokhlov and coworkers explored the assembly of such simulated PLCs in the bulk and at interfaces and evaluated various thermodynamic characteristics.[1−12]

The sequence along the copolymer compatibilizer has a profound effect on the phase behavior and interfacial characteristics of the blend to be compatibilized. Dadmun[13] used lattice Monte Carlo (MC) simulations based on the bond fluctuation model (BFM) to explore the effect of copolymer sequence distribution on the interfacial structure and miscibility of a compatibilized polymer blend containing a copolymer and two homopolymers. Dadmun considered block, alternating, random, random-alternating, and random-block copolymer sequences as compatibilizers. His results suggest that alternating and block copolymers represent the best interfacial modifiers, whereas random copolymers are the worst interfacial modifiers. Dadmun also reported that the departure of copolymer sequence from a purely random copolymer (i.e., random-alternating or random-block sequence) has a profound effect on the performance of the copolymer as an interfacial stabilizer. Using the BFM MC approach, Kamath and Dadmun[14] further explored the effect of the copolymer chain architecture on the dynamics of a binary blend formed by dispersing AB copolymers in a homopolymer A. They considered random, random-blocky, block, and alternating AB copolymer sequences and found that random and random-blocky copolymers are ideal compatibilizers because they move rapidly through the matrix phase within which they distribute uniformly. Using lattice MC simulations Ko et al.[15] examined the effect of compatibilizer sequence distribution on the phase separation dynamics of binary blends. They established that block copolymers possessed the best ability to retard the phase separation, whereas random compatibilizers outperformed alternating copolymers. Balazs and DeMeuse[16] extended the formalism of the Flory−Huggins theory and calculated the effect of the copolymer sequence on the phase diagrams for homopolymer A/homopolymer B/copolymer AB ternary systems at different copolymer concentrations. They reported that diblock copolymers were not always the optimal thermodynamic compatibilizers for a blend. Lyatskaya et al.[17] employed numerical self-consistent mean field methods to calculate the reduction in interfacial tension upon adding copolymer compatibilizers of varied sequence to a binary blend. Their study revealed that for

*Corresponding author.

© 2010 American Chemical Society
Published on Web 05/04/2010

a fixed copolymer molecular weight, block copolymers were the best interfacial compatibilizers, but longer random copolymers outperformed shorter block copolymers in reducing the interfacial tension between incompatible homopolymer phases.

Since the introduction of the coloring scheme for preparing PLCs suggested by Khokhlov and coworkers,[1−3,18,19] several experimental studies have been conducted aimed at synthesizing random copolymers with tunable monomer sequence distributions (RCPs).[20−28] Recently Genzer and coworkers[28] synthesized poly(styrene-*co*-4-bromostyrene) (PBr_xS) RCPs by brominating polystyrene (PS) in solvents with varying degree of solubility. Whereas bromination below the theta temperature of the parent homopolymer resulted in the formation of blocky PBr_xS RCPs, bromination above the theta temperature resulted in the formation of random PBr_xS RCPs. Genzer et al. also found that the sequence distribution of 4-BrS in PBr_xS PLCs has a profound effect on interfacial properties (i.e., adsorption and desorption[28,29]) and bulk properties (i.e., coil dimension in solution and solution viscosity[30]).

To this point, most experimental and theoretical research on compatibilizers has focused on the performance of block, random, alternating, random-blocky and random-alternating copolymers as compatibilizers for incompatible homopolymers blends. The use of PLCs as potential compatibilizers for immiscible homopolymers blends has not been explored. Because for a given degree of polymerization and composition, PLCs are blockier than random, alternating, random-blocky, and random-alternating copolymers,[6] they are more likely to form entanglements with homopolymer rich phases. They are also more likely to weave back and forth across the interface, binding the two homopolymers phases together and thus acting as effective compatibilizers for incompatible binary blends. This work focuses on utilizing PLCs as interfacial compatibilizers.

In this article, we present the results of discontinuous molecular dynamics (DMD) computer simulations aimed at supporting the development of PLCs as compatibilizing agents for a polymer blend containing two incompatible homopolymers. The DMD simulations are performed on an incompatible binary blend containing 530 38-mers of homopolymer A and 530 38-mers of homopolymer B, mutually immiscible, to which a small number (~0.66%) of 38-mers containing equal number of A and B monomers in the copolymer are added. Diblock, alternating, random, and PLCs made of A and B units are considered to be copolymer compatibilizers. Initially, the ternary blend system is equilibrated at high temperature and slowly cooled so that the homopolymer phases separate and the A−B copolymers end up localizing at the interface. The density profiles and the orientation of the different copolymers at the interface are evaluated to investigate the mechanism by which the copolymers stabilize the interface. To establish the efficacy of the various copolymer sequences, the interfacial width of the binary (no-copolymer) as well as the ternary (compatibilized) blend is calculated. Because it is difficult to assess directly the number of entanglements made by the copolymer compatibilizer with the respective homopolymer phases, the average number of crossings made by the copolymer across the interface is calculated and used as a proxy for the number of copolymer−homopolymer entanglements. The design of the DMD simulation is inspired by the work of Dadmun[13] on the effect of the copolymer sequence distribution on the interfacial characteristics and miscibility of a blend containing two homopolymers. Following Dadmun's[13] work, very few copolymer chains were added to the compatibilized blend so that the incompatible homopolymers would phase separate, leading to the formation of a interface, and the copolymers would migrate to the interface. However, our work goes beyond that of Dadmun[13] because we have explored PLCs as potential compatibilizers and compared their performance with that of the block, alternating, and random copolymers. Because it is easier to delineate the copolymer sequence effects for longer chains, we have used 38-mer (close to the entanglement length[31,32]) polymer chains; both the copolymers and the homopolymers employed in Dadmun's[13] work were 10-mers. To gain better insight into the weaving effect of various copolymer sequences, we have estimated the average number of crossings made by the various copolymer sequences across the interface, the average crossing length, and the normalized number of crossings.

Highlights of our results are as follows. The two incompatible homopolymers, A and B, in the compatibilized blend phase separate upon annealing; the copolymers migrate to the A/B interface regardless of the copolymer sequence. The width of the density profile for block (A-*b*-B) copolymers across the interface is largest, followed by those for A−B PLCs, random (A-*co*-B), and alternating (A-*alt*-B) copolymers. The interfacial width of the ternary (compatibilized) blend for the various copolymer sequences is higher than the binary (no-copolymer) blend. The interfacial width of the block copolymer compatibilized blend is highest, followed by PLCs, random, and alternating copolymer compatibilized blends. The radius of gyration of the copolymer perpendicular ($\langle R_g^2 \rangle_\perp$) and parallel ($\langle R_g^2 \rangle_\parallel$) to the interface is evaluated and presented. Block copolymers stretch most across the interface, whereas alternating copolymers stretch the least across the interface. PLCs stretch more across the interface than random copolymers at $T^* \leq 2$, where T^* is a reduced temperature. Alternating copolymers stretch most along the interface, whereas block copolymers stretch the least along the interface. Random copolymers stretch more along the interface than PLCs at $T^* < 4$. The average number of crossings across the interface made by different copolymers is calculated. Alternating copolymers make the most number of crossings, followed by random, PLCs, and block copolymers. The average crossing length for block copolymers is highest, followed by those for PLCs, random, and alternating copolymers. To estimate the efficiency of the knitting effect of the copolymer; the average number of crossings across the interface is normalized by the number of junction points, that is, the number of bonds between A and B monomers in the AB copolymer. Apart from block copolymers, PLCs are very efficient in making multiple crossings across the interface compared with the other copolymer sequences investigated. The average number of crossings across the interface is as high as 80% of the total number of junction points for the PLCs, which suggests that high-molecular-weight PLCs might be very efficient in stabilizing the interface.

In the next section, we describe the DMD method and the generation of PLCs via the instant coloring procedure of Khokhlov and coworkers. The following section presents the simulation results for various copolymer sequences. The final section concludes with a short summary of the Results and Discussion.

Model and Method

The binary blend system consists of 530 38-mers of a chains and 530 38-mers of B chains. The ternary (compatibilized) blend consists of the binary blend plus 7 38-mers of copolymer chains containing monomers of types a and b with composition $x_A = x_B = 0.5$. The chain lengths for the homopolymer/copolymer are chosen as 38 because it is close to the entanglement length of the polymer chains present in the blend.[31,32] The number of copolymer chains is chosen to be low (7 or ~0.66%) to prevent compatibilization and to ensure the formation of a interface in the copolymer blend system at low reduced temperature after equilibrium is attained. Because in the phase-separated "compatibilized" blend the copolymers are likely to be present at the interface, we can make inferences about the relative efficiency of the copolymers by calculating several properties discussed later in this section. The copolymers and homopolymers are modeled

as flexible chains of nearly tangent spheres. To increase computational efficiency, we have chosen to have the two components A and B repel each other instead of having attractive A−A and attractive B−B interactions. Therefore, the A−A and B−B interactions are modeled using a hard sphere potential, whereas the incompatibility between A and B components is modeled as a repulsive square-shoulder potential of strength ε_{AB}, which extends to an intermolecular separation $\lambda\sigma$ with $\lambda = 1.5$. The resulting potentials are

$$U_{AA}(r) = U_{BB}(r) = \begin{cases} \infty \text{ if } r \le \sigma \\ 0 \text{ if } r > \sigma \end{cases} \quad (1)$$

$$U_{AB}(r) = \begin{cases} \infty \text{ if } r \le \sigma \\ \varepsilon_{AB} \text{ if } \sigma < r \le \lambda\sigma \\ 0 \text{ if } r > \lambda\sigma \end{cases} \quad (2)$$

The packing fraction, $\eta = \pi N\sigma^3/(6V)$, for the pure as well as compatibilized blend is set to $\eta = 0.35$, where N is the number of spheres in the simulation box and V is the volume of the simulation box.

In a DMD computer simulation, particles experience collisions when they encounter a discontinuity in the potential such as the boundary of a hard sphere, square well, or square shoulder potential. Between collisions, particles move along linear trajectories, making the simulation technique faster than traditional MD simulations. The postcollision velocities can be found by solving the collision dynamics equations. To treat chains of spheres effectively, Rapaport created bonds by restricting the distance between adjacent spheres along a chain to lie between σ and $\sigma(1 + \delta)$.[33,34] Bellemans later extended this model so that the distance between adjacent spheres is allowed to lie between $\sigma(1 - \delta/2)$ and $\sigma(1 + \delta/2)$, making the average bond length σ.[35] The temperature of the system and, concordantly, the total kinetic energy are held constant throughout the DMD simulation. To regulate temperature, we employ a heat bath in the form of an Andersen thermostat,[36] which allows the temperature to fluctuate about an average system temperature, $T^* \equiv k_BT/\varepsilon_{AB}$. This is accomplished by having spheres collide stochastically with "ghost" particles, which then change the spheres' velocity.

To characterize statistically the different types of AB copolymer sequences used as compatibilizers, we need to introduce the uniformity factor developed by Dadmun.[13] The uniformity factor for component A is defined as

$$U_A = ([\sum_{l=1}^{L-1} s_l] + 1)/(L_A - 1) \quad (3)$$

where s_l is 1 if the lth and $(l+1)$-st sphere are type A, -1 if the lth sphere is type A and the $(l+1)$-st sphere is B type, and 0 if the lth sphere is B type regardless of the type of $(l+1)$-st sphere. Here L is the total number of monomers in the copolymer and L_A is the total number of A spheres in the copolymer. By definition, compositionally symmetric (50% A, 50% B) alternating copolymers have uniformity factor -1, symmetric block copolymers have uniformity factor 1, and symmetric random copolymers have uniformity factor 0. The uniformity factor for symmetric PLCs should lie roughly halfway between those for random and block copolymers.

The symmetric random AB copolymer was generated using the following algorithm. Starting with a homopolymer A, spheres were picked randomly and changed to type B if the sphere chosen was of type A. This process was repeated until the desired composition was achieved and the uniformity factor for components A and B in the random AB copolymer sequence was reduced to zero.

The symmetric AB 38-mer PLCs were generated via a simulation-based instantaneous coloring procedure originally proposed by Khokhlov et al.[1−3] A 38-mer A chain with square well interactions (well width $\lambda_{AA} = 1.5$) between non adjacent A spheres was initialized in a random coil configuration. Figure 1a shows that the initial configuration. DMD simulations were performed on the 38-mer A chain at a low reduced temperature $T^* = k_BT/|\varepsilon_{AA}| = 1.0$. The simulation box was chosen to be big enough (box length 15) so that the isolated chain did not interact with its periodic images. The chain collapsed to a globular conformation after ~1 million DMD moves. Figure 1b shows a snapshot of the resulting globular conformation. The spheres in the final globular conformation were sorted in order of their distance from the center of the globule. The 19 spheres farthest from the center were colored to be B, as depicted in Figure 1c. The coloring procedure resulted in the creation of an AB PLC with composition $x_A = x_B = 0.5$. After the coloring procedure, the AB PLC was relaxed. Figure 1d shows a snapshot of the symmetric AB 38-mer PLC generated via the instantaneous coloring procedure. Figure 2 illustrates the four copolymer sequences considered: (a) block, (b) random, (c) alternating, and (d) PLCs.

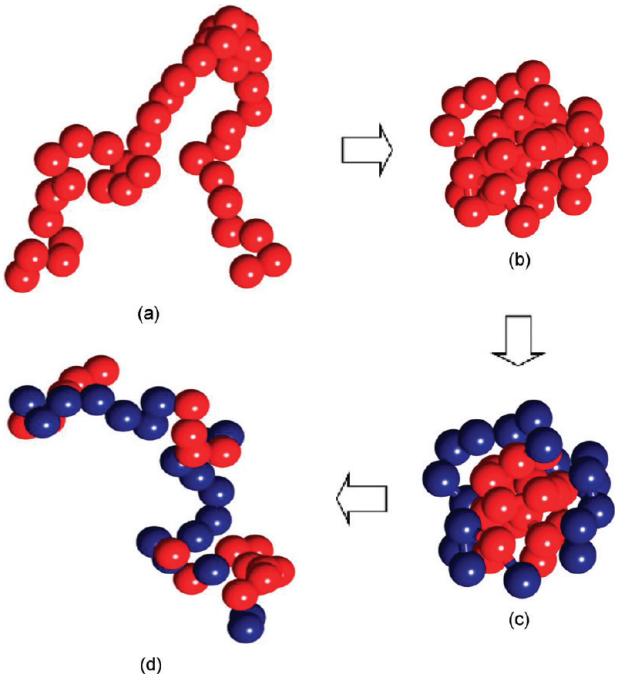

Figure 1. Snapshots illustrating instantaneous coloring procedure to generate 38-mer AB PLC (A = red, B = dark blue) with composition $x_A = x_B = 0.5$: (a) random configuration of 38-mer A chain, (b) collapsed globular configuration of the A chain, (c) 19 spheres farthest from the center of the globule are colored to type B, and (d) relaxed chain configuration of the resulting AB PLC.

DMD simulations were performed on the binary and ternary blend systems. The simulations on the blend systems were started in a random configuration at the desired packing fraction. Both blend systems were relaxed at an initial high temperature $T^* = 20$ and then annealed slowly in steps of $\Delta T^* = 1$ until $T^* = 1$ was achieved. At each temperature, DMD simulations were performed for 6 billion moves to allow for sufficient equilibration of the system.

The morphology and interfacial characteristics of the blend were characterized via the following measures: (1) the density profiles of homopolymers A and B and the copolymer with respect to the interface, (2) the interfacial width of the binary (no-copolymer) and the ternary compatibilized blend, (3) the radius of gyration of the copolymer perpendicular to the interface, $\langle R_g^2\rangle_\perp$, (4) the radius of gyration of the copolymer parallel to the interface, $\langle R_g^2\rangle_\parallel$, (5) the shape anisotropy of the copolymer coil, defined here as $\alpha = \langle R_g^2\rangle_\parallel - \langle R_g^2\rangle_\perp$, (6) the average number of crossings made by the copolymer across the interface, $< N_t >$, (7) the

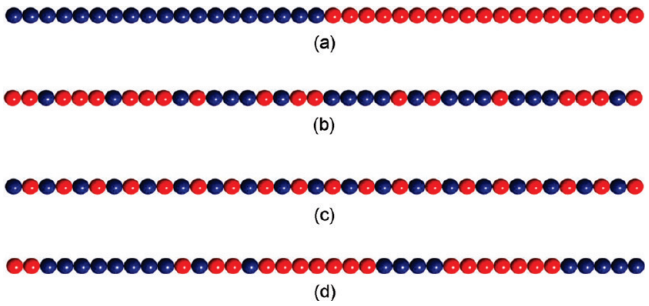

Figure 2. Sequences of 38-mer AB copolymers (A = red, B = dark blue) with composition $x_A = x_B = 0.5$: (a) block, (b) random (one sequence realization), (c) alternating, and (d) PLC (one sequence realization).

average length of a crossing made by the copolymer across the interface, and (8) the normalized number of crossings made by the copolymer across the interface, $< L_t >$.

We use the density profiles of homopolymer A, homopolymer B, and copolymer AB to calculate the interfacial width of the binary (no-copolymer) as well as the ternary (compatibilized) blend utilizing the approach developed by Helfand and coworkers.[37−40] Under the Helfand approach, the interfacial width for the binary and ternary blend is defined by the following formulas

$$w_{AB} = \int_{-\infty}^{\infty} \Phi_A(x)\Phi_B(x)\,dx \tag{4}$$

$$w_{ABC} = \int_{-\infty}^{\infty} \{\Phi_A(x)\Phi_B(x) + \Phi_A(x)\Phi_C(x) + \Phi_B(x)\Phi_C(x)\}\,dx \tag{5}$$

where w_{AB} and w_{ABC} are the interfacial width of the binary (no-copolymer) and ternary (compatibilized) blend, respectively. $\Phi_A(x)$, $\Phi_B(x)$, and $\Phi_C(x)$ are local volume fractions of the homopolymer A, homopolymer B, copolymer AB, respectively, and x in the direction perpendicular to the A/B interface.

The radius of gyration of the copolymer perpendicular and parallel to the interface is defined by the following formulas

$$\langle R_g^2 \rangle_\perp = \sum_{i=1}^{N}\sum_{j=1}^{L}\sum_{k=1}^{L}\{r(i,j)_\perp - r(i,k)_\perp\}^2/\{2(L)^2N\} \tag{6}$$

$$\langle R_g^2 \rangle_{||} = \sum_{d=1}^{2}\sum_{i=1}^{N}\sum_{j=1}^{L}\sum_{k=1}^{L}\{r(i,j)_{||}^d - r(i,k)_{||}^d\}^2/\{4(L)^2N\} \tag{7}$$

Here $r(i,j)_\perp$ is the position of the jth monomer on the ith copolymer chain along the direction perpendicular to the interface and $r(i,j)_{||}$ is the position of the jth monomer on the ith copolymer chain along the direction parallel to the interface, N is the number of copolymer chains, L is the number of spheres in a single copolymer chain, d refers to the two directions parallel to the interface in the phase-separated regime of the compatibilized blend. Equations 6 and 7 for $\langle R_g^2 \rangle_\perp$ and $\langle R_g^2 \rangle_{||}$ are mathematically equivalent to the formula for the radius of gyration involving the center of mass. The anisotropy of the copolymer chain is characterized by the parameter α which is defined to be

$$\alpha = \langle R_g^2 \rangle_{||} - \langle R_g^2 \rangle_\perp \tag{8}$$

The average number of crossings, $< N_t >$, at a given temperature is calculated by locating the interface in the phase-separated compatibilized blend after equilibrium is attained, calculating the number of times a copolymer chain intersects the interface followed by averaging over all of the copolymer chains. The average length of the crossing ($< L_t >$) across the interface for a copolymer is defined as $< L_t > = L/(< N_t > + 1)$, where L is the length of the copolymer and $< N_t >$ is the average number of crossings across the interface made by the copolymer.

The system properties for both the binary and ternary blend systems were averaged over five runs starting from uncorrelated random initial configurations. The results for ternary blends compatibilized by PLCs or random copolymer were averaged over 10 different copolymer sequences for a given initial configuration. Therefore, 50 simulations were performed for ternary blends compatibilized by either PLCs or random copolymer. The error bars depicted for each graph represent the sample standard deviations of the properties calculated and plotted on the graphs.

Results and Discussion

Snapshots of the symmetric binary blend system are shown in Figure 3. Figure 3a shows that the binary blend is homogeneous at initial high temperature $T^* = 20$. After the binary blend is annealed to low temperature $T^* = 1$, the two incompatible homopolymers have phase separated, forming an interface (cf. Figure 3b). Snapshots of the ternary blend with PLCs as the compatibilizing agent are shown in Figure 4. Specifically, Figure 4a demonstrates that the compatibilized blend is initially homogeneous at $T^* = 20$. After lowering the system temperature to $T^* = 1$, the two incompatible homopolymers have phase separated, forming an interface with PLCs localized at the interface (cf. Figure 4b). Similar trends are observed for the other compatibilized blend systems containing block, alternating, and random copolymers. To locate the direction of phase separation, the concentration distribution of components A and B along the three directions are regularly monitored during the simulation of the binary and ternary blend systems. At high temperatures, the components A and B in the blend are distributed uniformly. At lower temperatures, as the phase separation occurs, the concentration distribution of components A and B along the direction of phase separation is nonuniform, unlike those in the other two directions. Once the direction of phase separation has been established for the blend systems in the phase-separated regime, the interface can be located by calculating the gradient of the concentration distribution of components A and B along the direction of phase separation.

Figure 5 shows the density profiles of the two homopolymers and copolymer from the four compatibilized blends with ~0.66% (a) block, (b) random, (c) alternating, and (d) PLCs at $T^* = 1$ along the direction of phase separation. All copolymer sequences end up localizing at the interface, thereby stabilizing the interface. None of the copolymer sequences act as thermodynamic compatibilizers as intended; that is, they are unable to prevent the phase separation of the incompatible homopolymers because the amount of copolymer added is intentionally very low (~0.66%). Because of the periodic boundary conditions, there are two interfaces present in the system. The width of the density profile for block copolymers across the interface is highest, followed by those for PLCs, random, and alternating copolymers. The wider the density profile of the copolymer across the interface, the more the copolymer penetrates the homopolymer-rich phases, leading to entanglements and better interfacial strength. Figure 6 shows the interfacial width of the binary (no-copolymer) and ternary (compatibilized) blend as a function of the reduced temperature. The interfacial width of the compatibilized blend for the various copolymer sequences is higher than the binary blend, which clearly shows that all four copolymer compatibilizers act as effective interfacial stabilizers. The interfacial width of block copolymers is highest, followed by PLCs, random, and alternating copolymers.

To act as an effective interfacial modifier, a copolymer compatibilizer must migrate to the interface and weave across the interface, thus promoting adhesion between the immiscible phases by knitting them together. Therefore, an ideal copolymer compatibilizer

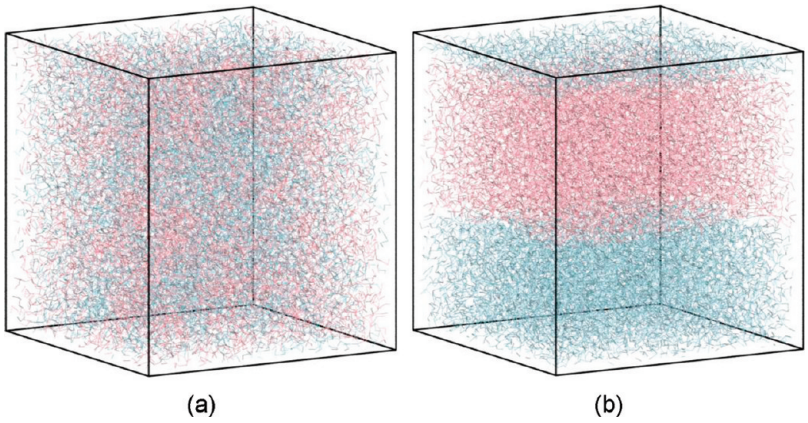

Figure 3. Simulation snapshots of the binary blend in: (a) initial configuration at $T^* = 20$ and (b) phase-separated configuration at $T^* = 1$.

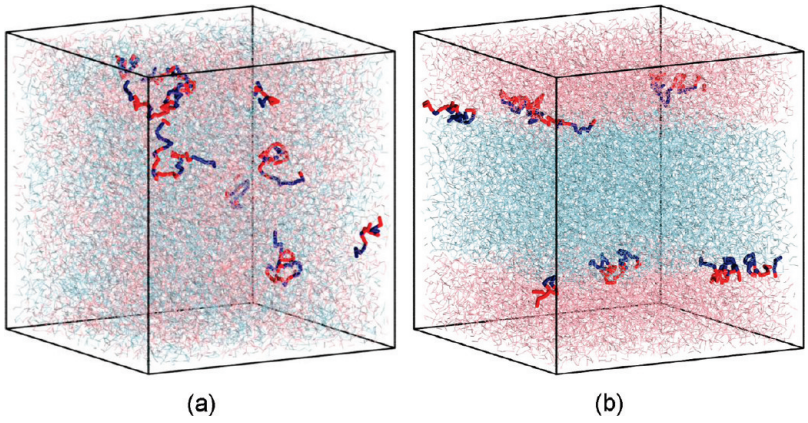

Figure 4. Simulation snapshots of PLC compatibilized blend in: (a) initial configuration at $T^* = 20$ and (b) phase-separated configuration at $T^* = 1$.

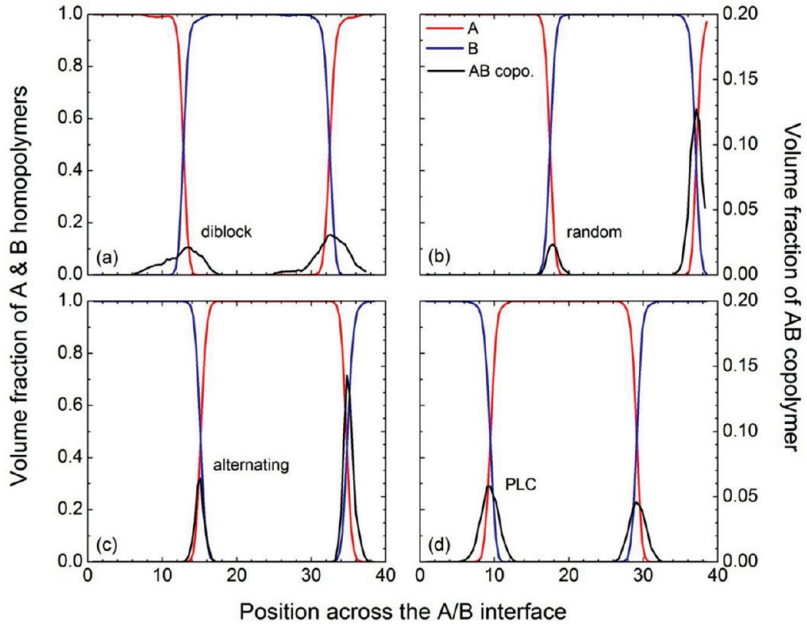

Figure 5. Density profiles for the homopolymers (red and blue lines) and copolymer (black lines) in the compatibilized blend at $T^* = 1$: (a) block, (b) random, (c) alternating, and (d) PLC.

is one that maximizes the number of entanglements it makes with the homopolymers on either side of the interface. Because it is difficult to quantify directly the number of entanglements made by the copolymer with the homopolymer, an alternative way is to look at the orientation of the copolymer with respect to the interface via the radius of gyration parallel and perpendicular to the interface and the average number of crossings made by the copolymer across the interface. If the copolymer is stretched sufficiently perpendicular to (and spaced well parallel across) the interface, thus making numerous crossings across the interface, then it is more likely to form entanglements with the homopolymers and act as an effective interfacial modifier.

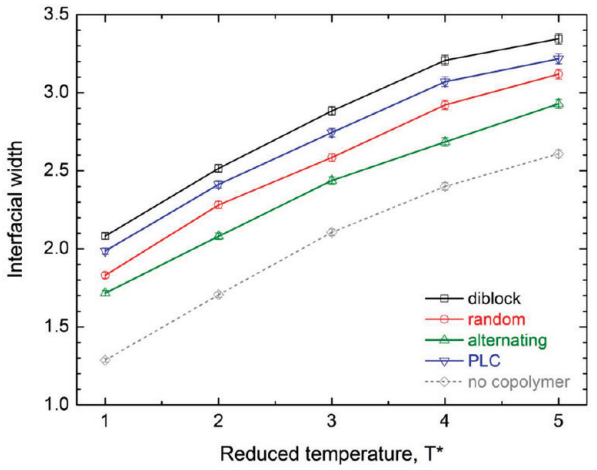

Figure 6. Interfacial width versus the reduced temperature of the binary (no-copolymer) and ternary (compatibilized) blend.

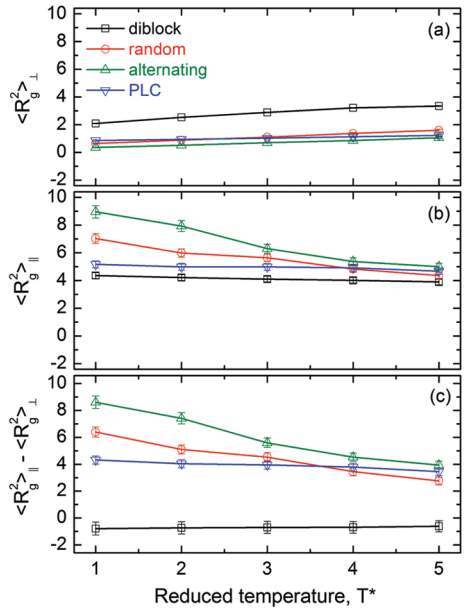

Figure 7. (a) Radius of gyration of the copolymer perpendicular to the interface versus the reduced temperature, (b) radius of gyration of the copolymer parallel to the interface versus the reduced temperature, and (c) anisotropy of the copolymer, $\langle R_g^2\rangle_\parallel - \langle R_g^2\rangle_\perp$, versus the reduced temperature for the different copolymer sequences.

The orientation of the copolymer at the interface depends upon the sequence of the copolymer and the temperature. Figure 7a shows the radius of gyration of the copolymer perpendicular to the interface $\langle R_g^2\rangle_\perp$ versus the reduced temperature for the four copolymer compatibilizers. Block copolymers stretch most across the interface, whereas alternating copolymers stretch least. PLCs penetrate the interface more than random copolymers at $T^* \leq 2$. The reason for this switching behavior between PLCs and random copolymer is unclear. Therefore, block copolymers stabilize the interface by penetrating into the homopolymer phase on either side of the interface, allowing the formation of entanglements and the reduction of unfavorable contacts. Figure 7b shows the radius of gyration of the copolymer parallel to the interface $\langle R_g^2\rangle_\parallel$ versus the reduced temperature for the four copolymer compatibilizers. Alternating copolymers stretch most along the interface, whereas block copolymers stretch least. Random copolymers stretch more along the interface than PLCs at $T^* < 4$. The reason for this switching behavior between PLCs and random copolymer is

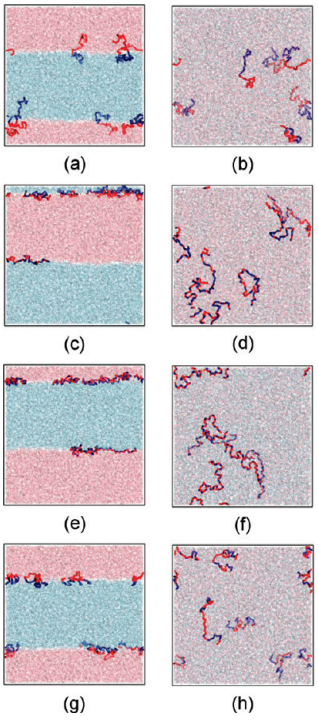

Figure 8. Simulation snapshots of the compatibilized blend after equilibrium has been attained at $T^* = 1$: (a) block (side view of the simulation box parallel to the interface), (b) block (top view of the simulation box perpendicular to the interface), (c) random (side view), (d) random (top view), (e) alternating (side view), (f) alternating (top view), (g) PLC (side view), and (h) PLC (top view).

unclear. At any given temperature, $\langle R_g^2\rangle_\perp$ is greater than $\langle R_g^2\rangle_\parallel$ for the block copolymer, which implies that the block copolymer volume is shaped like a cylinder driven into the interface. Because the diblock copolymer barely covers the interface, each of the two blocks of the diblock copolymer adopts a mushroom-type configuration. At a given temperature for alternating, random, and PLCs, $\langle R_g^2\rangle_\parallel$ is greater than $\langle R_g^2\rangle_\perp$, which suggests that copolymer volumes for these sequences are shaped like a pancake.

The preferred orientation of the copolymer with respect to the interface can be characterized by the anisotropy, as measured by the parameter α previously defined. Figure 7c shows a plot of α versus the reduced temperature for the four copolymer sequences. Anisotropy increases as temperature decreases for all four copolymer compatibilizers, revealing that as the thermal fluctuations decrease, the copolymers adopt a preferred lower energy configuration at the interface. Alternating copolymers are most anisotropic, whereas block copolymers are least anisotropic. Random copolymers are more anisotropic than PLCs at $T^* \leq 3$. The reason for this switching behavior between PLCs and random copolymer is unclear at the moment.

Figure 8 depicts the side view of the simulation box parallel to the interface (left panel) as well as the top view of the simulation box perpendicular to the interface (right panel) for each of the four compatibilized blends with ~0.66% copolymer after equilibrium has been attained at $T^* = 1$. Block copolymers (Figures 8a,b) orient preferentially perpendicular to the interface penetrating the homopolymer phases on either side of the interface. Alternating copolymers (Figures 8e,f) prefer to lie parallel to the interface. Random copolymers (Figures 8c,d) and PLCs (Figures 8g,h) also prefer to lie parallel to the interface, although to a lesser degree than alternating copolymers.

Because the primary mechanism for interfacial compatibilization of the immiscible homopolymer blends containing random, alternating, and PLC is knitting across the interface, the average

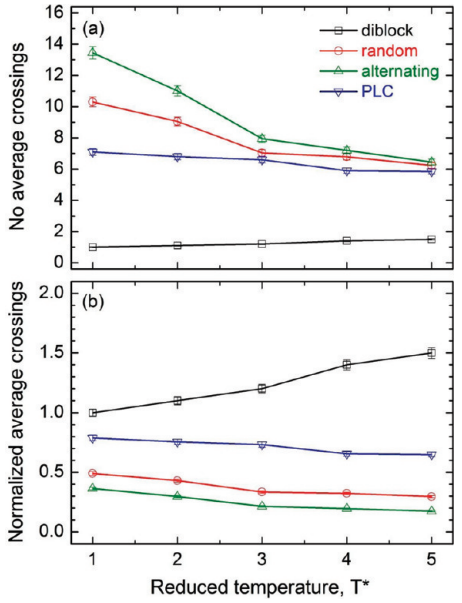

Figure 9. (a) Average crossings made by the different copolymer types across the interface versus the reduced temperature and (b) normalized average crossings (average crossings made by the different copolymer types across the interface divided by the number of junction points in the copolymer) versus the reduced temperature.

number of crossings made by the different copolymers across the interface is an important factor in determining the relative performance of the copolymer sequences as effective compatibilizers. Figure 9a depicts the average number of crossings across the interface as a function of the reduced temperature for the four copolymer sequences. Alternating copolymers make the highest average number of crossings across the interface, followed by random, PLCs, and block copolymers. These findings are consistent with the fact that alternating copolymers stretch most along the interface (i.e., $\langle R_g^2 \rangle_\parallel$ is high) and have the highest number of junction points for a given degree of polymerization and composition of the copolymer, that is, the number of bonds between A and B monomers in the AB copolymer. Block copolymers make a single crossing across the interface because they have just one junction point. Random copolymers make more crossings across the interface than PLCs as they have a higher number of junction points than PLCs. At $T^* = 1$, the average length of the crossing for the different copolymers is: block ($38/2 \approx 19$), alternating ($38/14.5 \approx 2.6$), random ($38/11.5 \approx 3.3$), and PLCs ($38/8 \approx 4.8$). Apart from diblock copolymers, PLCs have the highest average crossing length. When the average number of crossings across the interface is normalized by the number of junction points in the copolymer, an interesting trend arises. Figure 9b shows the normalized number of crossings across the interface versus the reduced temperature for the four copolymer sequences. Apart from diblock copolymers, PLCs are very efficient in making multiple crossings across the interface compared with any other copolymer sequences. The average number of crossings across the interface for PLCs is as high as 80% of the number of junction points for the PLC, which suggests that high-molecular-weight PLC might be very efficient in stabilizing the interface.

Our results are in good agreement with the lattice MC simulations of Dadmun[13] for block, random, and alternating copolymers. The simulation results from Dadmun's work on random-block (uniformity factor of 0.5) copolymers cannot be extended directly to PLCs for comparison because random-block copolymers have a sequence distribution different than PLCs. Moreover, the copolymer chains used (10-mer) in Dadmun's work were shorter (below the entanglement length), and it is certainly easier to detect sequence effects accurately for longer copolymer chains. Further support for this is Khokhlov's[6] demonstration that random-block copolymers (whose block length obeys a Poisson distribution) are statistically different from PLCs (which obey Levy flight statistics for the block length), despite having the same composition and average block length (or uniformity factor) for both types of copolymers. Although we have conducted the computationally intensive simulations for only one copolymer concentration (~0.66% at which the copolymers barely saturate the interface), we believe that the general trends among the various copolymer sequences hold true even at higher copolymer concentrations. Further studies of blends with higher copolymer concentrations are in progress and will be the subject of future publications.

Conclusions

We have performed DMD simulations aimed at supporting the development of PLCs as compatibilizing agents for a polymer blend containing two incompatible homopolymers. The results are compared with those for systems with block, alternating, and random copolymers acting as compatibilizers. As the compatibilized blend was annealed from high to low temperature, the two incompatible homopolymers phase separated, and the copolymers migrated to the interface. None of the added copolymers prevented the phase separation because the amount of copolymer added (~0.66%) was intentionally too low. We calculated the density profiles of the copolymer and homopolymers in the compatibilized blend along the direction of phase separation. The width of the density profile for block copolymers across the interface was highest, followed by those of PLCs, random, and alternating copolymers. The wider the density profile of the copolymer across the interface, the more the copolymer penetrates the homopolymer-rich phases leading to entanglements and better interfacial strength. We also calculated the interfacial width of the binary (no-copolymer) and ternary (compatibilized) blend. The interfacial width of the compatibilized blend for the various copolymer sequences is higher than the binary blend, which clearly shows that all four copolymer compatibilizers act as effective interfacial stabilizers. The interfacial width of block copolymers is highest, followed by PLCs, random, and alternating copolymers.

The orientation of the copolymer at the interface depended upon the sequence of the copolymer. The radii of gyration of the copolymer perpendicular ($\langle R_g^2 \rangle_\perp$) and parallel ($\langle R_g^2 \rangle_\parallel$) to the interface were monitored. Block copolymers stretched most across the interface, whereas alternating copolymers stretched least. PLCs stretched more across the interface than random copolymers at $T^* \leq 2$. Alternating copolymers stretched most along the interface, whereas block copolymers stretched least. Random copolymers stretched more along the interface than PLCs at $T^* < 4$. The reason why the orientation of PLCs relative to random copolymers switches as we reduce the temperature is unclear at the moment.

To gain deeper insight into the interfacial behavior and relative compatibilizing efficiency of the various copolymer sequences, the average number of crossings across the interface made by different copolymers was calculated. Because alternating copolymers have the highest number of junction points across the interface, they make the largest average number of crossings, followed by random, PLCs, and block copolymers. The average crossing length for block copolymers was highest, followed by those for PLCs, random, and alternating copolymers. The average number of crossings across the interface was normalized by the number of junction points to estimate the efficiency of the knitting effect of the copolymer. Apart from block copolymers,

PLCs were very efficient in making multiple crossings across the interface compared with the other copolymer sequences. The average number of crossings across the interface for PLCs was as high as 80% of the number of junction points for the PLC, which suggests that high-molecular-weight PLCs might be very efficient in stabilizing the interface.

The results of our simulation are in good agreement with the MC simulations of Dadmun[13] for block, random, and alternating copolymers. In a nutshell, sequence distribution in copolymer compatibilizers plays an important role in the way that these copolymers orient at the interface. PLCs penetrate the interface more than random and alternating copolymers at lower reduced temperatures and are very efficient in making multiple crossings across the interface. PLCs can be synthesized and tuned[28] easily, and hence they might be useful as potential compatibilizers and adhesion promoters for incompatible homopolymer blends. The contrast in the performance between PLCs and random copolymers as compatibilizers would be even better for longer chains, but the simulations become too computationally intensive for us to perform. A study of the dynamics of phase separation of PLC compatibilizers in blends is under way in our laboratory using kinetic lattice MC (BFM) simulations.

Acknowledgment. This work was supported by the Director, Office of Energy Research, Office of Basic Sciences, Chemical Science Division of the U.S. Department of Energy under grant DE-FG05-91ER14181 awarded to C.K.H. J.G. thanks the National Science Foundation for financial support through grant nos. DMR-0353102 and OISE-0730243.

References and Notes

(1) Khokhlov, A. R.; Khalatur, P. G. Conformation-dependent sequence design (engineering) of AB copolymers. *Phys. Rev. Lett.* **1999**, *82*, 3456–3459.
(2) Khalatur, P. G.; Ivanov, V. A.; Shusharina, N. P.; Khokhlov, A. R. Protein-like copolymers: computer simulation. *Russ. Chem. Bull.* **1998**, *47*, 855–860.
(3) Khokhlov, A. R.; Khalatur, P. G. Protein-like copolymers: computer simulation. *Phys. A* **1998**, *249*, 253–261.
(4) Zheligovskaya, E. A.; Khalatur, P. G.; Khokhlov, A. R. Properties of AB copolymers with a special adsorption-tuned primary structure. *Phys. Rev. E* **1999**, *59*, 3071–3078.
(5) Chertovich, A. V.; Ivanov, V. A.; Lazutin, A. A.; Khokhlov, A. R. Sequence design of biomimetic copolymers: Modeling of membrane proteins and globular proteins with active enzymatic center. *Macromol. Symp.* **2000**, *160*, 41–48.
(6) Govorun, E. N.; Ivanov, V. A.; Khokhlov, A. R.; Khalatur, P. G.; Borovinsky, A. L.; Grossberg, A. Yu. Primary sequences of proteinlike copolymers: Levy-flight-type long-range correlations. *Phys. Rev. E* **2001**, *64*, 040903.
(7) Kriksin, Y. A.; Khalatur, P. G.; Khokhlov, A. R. Reconstruction of protein-like globular structure for random and designed copolymers. *Macromol. Theory Simul.* **2002**, *11*, 213–221.
(8) van den Oever, J. M. P.; Leermakers, F. A. M.; Fleer, G. J.; Ivanov, V. A.; Shusharina, N. P.; Khokhlov, A. R.; Khalatur, P. G. Coil-globule transition for regular, random, and specially designed copolymers: Monte Carlo simulation and self-consistent field theory. *Phys. Rev. E* **2002**, *65*, 041708.
(9) Zherenkova, L. V.; Talitskikh, S. K.; Khalatur, P. G.; Khokhlov, A. R. Self-organization of quasi-random copolymers. *Dokl. Phys. Chem.* **2002**, *382*, 23–26.
(10) Velichko, Y. S.; Khalatur, P. G.; Khokhlov, A. R. Molecular dispenser: conformation-dependent design approach. *Macromolecules* **2003**, *36*, 5047–5050.
(11) Vasilevskaya, V. V.; Klochkov, A. A.; Lazutin, A. A.; Khalatur, P. G.; Khokhlov, A. R. HA (hydrophobic/amphiphilic) copolymer model: coil-globule transition versus aggregation. *Macromolecules* **2004**, *37*, 5444–5460.
(12) Khokhlov, A. R.; Khalatur, P. G. Biomimetic sequence design in functional copolymers. *Curr. Opin. Solid State Mater. Sci.* **2004**, *8*, 3–10.
(13) Dadmun, M. Effect of copolymer architecture on the interfacial structure and miscibility of a ternary polymer blend containing a copolymer and two homopolymers. *Macromolecules* **1996**, *29*, 3868–3874.
(14) Kamath, S. Y.; Dadmun, M. D. The effect of chain architecture on the dynamics of copolymers in a homopolymer matrix: Lattice Monte Carlo simulations using the bond-fluctuation model. *Macromol. Theory Simul.* **2005**, *14*, 519–527.
(15) Ko, M. J.; Kim, S. H.; Jo, W. H. The effects of copolymer architecture on phase separation dynamics of immiscible homopolymer blends in the presence of copolymer: a Monte Carlo simulation. *Polymer* **2000**, *41*, 6387–6394.
(16) Balazs, A. C.; DeMeuse, M. T. Miscibility in ternary mixtures containing a copolymer and two homopolymers. Effect of sequence distribution. *Macromolecules* **1989**, *22*, 4260–4267.
(17) Lyatskaya, Y.; Gersappe, D.; Balazs, A. C. Effect of copolymer architecture on the efficiency of compatibilizers. *Macromolecules* **1995**, *28*, 6278–6283.
(18) Chertovich, A. V.; Govorun, E. N.; Ivanov, V. A.; Khalatur, P. G.; Khokhlov, A. R. Conformation-dependent sequence design: evolutionary approach. *Eur. Phys. J. E* **2004**, *13*, 15–25.
(19) Chertovich, A. V.; Ivanov, V. A.; Zavin, B. G.; Khokhlov, A. R. Conformation-dependent sequence design of HP copolymers: an algorithm based on sequential modifications of monomer units. *Macromol. Theory Simul.* **2002**, *11*, 751–756.
(20) Virtanen, J.; Baron, C.; Tenhu, H. Grafting of poly(*N*-isopropylacrylamide) with poly(ethylene oxide) under various reaction conditions. *Macromolecules* **2000**, *33*, 336.
(21) Virtanen, J.; Tenhu, H. Thermal properties of poly(*N*-isopropylacrylamide)-*g*-poly(ethyl oxide) in aqueous solutions: influence of the number and distribution of the grafts. *Macromolecules* **2000**, *33*, 5970.
(22) Virtanen, J.; Lemmetyinen, H.; Tenhu, H. Fluorescence and EPR studies on the collapse of poly(*N*-isopropyl acrylamide)-*g*-poly(ethylene oxide) in water. *Polymer* **2001**, *42*, 9487.
(23) Wahlund, P.-O.; Galaev, I. Y.; Kazakov, S. A.; Lozinsky, V. I.; Mattiasson, B. Protein-like copolymers: effect of polymer architecture on the performance in bioseparation process. *Macromol. Biosci.* **2002**, *2*, 33.
(24) Lozinsky, V. I.; Simenel, I. A.; Semenova, M. G.; Belyakova, L. E.; Il'in, M. M.; Grinberg, V. Ya.; Dubovik, A. S.; Khokhlov, A. R. Behavior of protein-like *N*-vinylcaprolactam and *N*-vinylimidazole copolymers in aqueous solutions. *Vysokomol. Soedin., Ser. A* **2006**, *48*, 435–443.
(25) Lozinsky, V. I.; Simenel, I. A.; Kulakova, V. K.; Kurskaya, E. A.; Babushkina, T. A.; Klimova, T. P.; Burova, T. V.; Dubovik, A. S.; Grinberg, V. Ya.; Galaev, I. Yu.; Mattiasson, B.; Khoklov, A. R. Synthesis and studies of *N*-vinylcaprolactam/*N*-vinylimidazole copolymers that exhibit the "proteinlike" behavior in aqueous media. *Macromolecules* **2003**, *36*, 7308–7323.
(26) Lozinsky, V. I.; Ivanov, R. V.; Kalinina, E. V.; Timofeeva, G. I.; Khokhlov, A. R. Redox-initiated radical polymerisation of acrylamide in moderately frozen water solutions. *Macromol. Rapid Commun.* **2001**, *22*, 1441–1446.
(27) Lozinsky, V. I.; Simenel, I. A.; Kurskaya, E. A.; Kulakova, V. K.; Galaev, I. Yu.; Mattiasson, B.; Grinberg, V. Ya.; Grinberg, N. V.; Khokhlov, A. R. Synthesis of *N*-vinylcaprolactam polymers in water-containing media. *Polymer* **2000**, *41*, 6507–6518.
(28) Semler, J. J.; Jhon, Y. K.; Tonelli, A.; Beevers, M.; Krishnamoorti, R.; Genzer, J. Facile method of controlling monomer sequence distributions in random copolymers. *Adv. Mater.* **2007**, *19*, 2877–2883.
(29) Han, J.; Jeon, B. H.; Ryu, C. Y.; Semler, J. J.; Jhon, Y. K.; Genzer, J. Discriminating among co-monomer sequence distributions in random copolymers using interaction chromatography. *Macromol. Rapid Commun.* **2009**, 1543–1548.
(30) Semler, J. J. Ph.D. Thesis, NC State University, **2003**.
(31) Smith, S. W.; Hall, C. K.; Freeman, B. D. Molecular dynamics study of entangled hard-chain fluids. *J. Chem. Phys.* **1996**, *104*, 5616–5637.
(32) Smith, S. W.; Hall, C. K.; Freeman, B. D. Large-scale molecular-dynamics study of entangled hard-chain fluids. *Phys. Rev. Lett.* **1995**, *75*, 1316–1319.
(33) Rapaport, D. C. Molecular dynamics simulation of polymer chains with excluded volume. *J. Phys. A* **1978**, *11*, L213.
(34) Rapaport, D. C. Molecular dynamics study of polymer chains. *J. Chem. Phys.* **1979**, *71*, 3299.

(35) Bellemans, A.; Orbans, J.; Belle, D. V. Molecular dynamics of rigid and non-rigid necklaces of hard disks. *Mol. Phys.* **1980**, *39*, 781–782.
(36) Andersen, H. C. Molecular dynamics simulations at constant pressure and/or temperature. *J. Chem. Phys.* **1980**, *72*, 2384–2393.
(37) Helfand, E. Theory of the homopolymer/binary-polymer mixture interface. *Macromolecules* **1992**, *25*, 1676–1685.
(38) Helfand, E.; Sapse, A. M. Theory of unsymmetric polymer-polymer Interfaces. *J. Chem. Phys.* **1975**, *62*, 1327.
(39) Helfand, E.; Tagami, Y. Theory of the interface between immiscible polymers. *Polym. Lett.* **1971**, *9*, 741–746.
(40) Helfand, E.; Tagami, Y. Theory of the interface between immiscible polymers. II. *J. Chem. Phys.* **1972**, *56*, 3592.